

ment²² of LiH by the method of *G1* orbitals yielded a value of $q/2e = -0.0202a_0^{-3}$ in agreement with the Browne-Matsen result for the undeformed core. Palke and Goddard observe that the two LiH inner-shell orbitals obtained according to the *G1* method are "essentially identical" to the *G1* inner-shell orbitals for a free Li atom; thus, this method fails to take account of core deformation.

Since $-0.0202a_0^{-3}$ appears to be a good value for $q_0/2e$, better than the result of $-0.0175a_0^{-3}$ obtained from our six-configuration wave function, the value of $q/2e = -0.0156a_0^{-3}$ obtained after applying the Sternheimer correction should be fairly reliable. This is to be compared with the results of the four direct

treatments in which the wave function explicitly provided for core deformation: $q/2e = -0.0166$ (Kahalas and Nesbet³), -0.0173 (Browne and Matsen⁴), -0.0182 (Bender and Davidson⁵), and $-0.0173a_0^{-3}$ (Bender and Davidson⁶). From these five values we estimate that the best current value of $q/2e$ is $(-0.0170 \pm 0.0013)a_0^{-3}$. The experimental result¹ for the nuclear quadrupole coupling constant is $eqQ/h = 346 \pm 1$ kc/sec from which the electric quadrupole moment Q of the Li⁷ nucleus is found to be $(-4.3 \pm 0.3) \times 10^{-26}$ cm². The implications for nuclear shell theory of a quadrupole moment of this magnitude have been previously discussed.²³

²³ R. D. Present, Phys. Rev. **139**, B300 (1965); B. M. Morris and R. D. Present, *ibid.* **140**, B1197 (1965).

Spin-Lattice Relaxation of Tm²⁺ in CaF₂, SrF₂, and BaF₂

E. S. SABISKY AND C. H. ANDERSON

RCA Laboratories, Princeton, New Jersey 08540

(Received 11 August 1969)

Measurements were made of the spin-lattice relaxation time of the ground state of Tm²⁺ in CaF₂, SrF₂, and BaF₂ over the magnetic field range of 1 to 12 kG and temperature range of 1.3 to 20°K. The one-phonon relaxation process was unambiguously identified by its characteristic fourth-power dependence on frequency and its linear temperature dependence. The Raman process with its T^9 dependence begins to dominate the relaxation above 5°K. The angular dependence of the relaxation permitted the separation of the effect of the two local modes, E_g and T_{2g} , on the one-phonon process. Calculations were in good agreement with theory, and they showed that the second-order terms of the orbit-lattice interaction dominate the relaxation process. Continuous measurement of the relaxation over this magnetic field range was made possible by a technique which is independent of any microwave sources. The detection was done by monitoring the magnetic circular dichroism of the broad optical absorption bands.

I. INTRODUCTION

SPIN-LATTICE relaxation times T_1 have been extensively studied for many paramagnetic impurities¹ in a variety of hosts. The theory for direct interactions between the individual spins and the lattice was first presented by Kronig² and Van Vleck.³ Mattuck and Strandberg⁴ along with others have re-examined the theory for the iron group ions while Orbach⁵ has considered the rare-earth group. Generally, the comparison between the experimental results and predictions is inconsistent. This is due to the experimental difficulties encountered in obtaining reliable data of the single-ion relaxation process and because of the theoretical complexity of the dynamic orbit-lattice interaction.

The linear variation of the relaxation rate with temperature as predicted for the one-phonon process has been observed by many authors.¹ The dependence of T_1^{-1} on the fourth power of magnetic field strength, predicted for direct relaxation of Kramer's ions by resonant phonons at a given temperature, has been observed in only a few cases.⁶ In this paper, we present⁷ extensive measurements of the spin-lattice relaxation rate of divalent thulium, a Kramer's ion, in the cubic hosts CaF₂, SrF₂, and BaF₂. The direct one-phonon process is well demonstrated in all three hosts by both temperature- and frequency-dependent measurements. Because this is a simple system, these measurements provide a good basis for comparison with theory. It is the most complete verification to date of the H^4T term in Van Vleck's theory for the one-phonon relaxation process.

¹ For a collection of papers, see *Spin-Lattice Relaxation in Ionic Solids*, edited by A. A. Manenkov and R. Orbach (Harper and Row Publishers, Inc., New York, 1966).

² R. de L. Kronig, Physica **6**, 33 (1939).

³ J. H. Van Vleck, J. Chem. Phys. **7**, 72 (1939); Phys. Rev. **57**, 426 (1940).

⁴ R. D. Mattuck and M. W. P. Strandberg, Phys. Rev. **119**, 1204 (1960).

⁵ R. Orbach, Proc. Roy. Soc. (London) **A264**, 456 (1961).

⁶ Douglas A. Davids and Peter E. Wagner, Phys. Rev. Letters **12**, 141 (1964); N. E. Kask, Fiz. Tverd. Tela **8**, 1129 (1966) [English transl.: Soviet Phys.—Solid State **8**, 900 (1966)]; H. Panepucci and L. F. Mollenauer, Phys. Rev. **178**, 589 (1969).

⁷ A brief account of this work was presented at the May 1968 meeting of the American Physical Society, Bull. Am. Phys. Soc. **13**, 621 (1968).

The experimental techniques⁸ used are based primarily on optical detection of the spin orientation, which is possible because of the strong circular dichroism in the broad absorption bands of this ion. This enabled us to lift the restriction of operating only at those frequencies obtainable in a conventional microwave system. The methods employed permitted easy operation at any obtainable Zeeman splitting.

These studies are important not only because of the insights they provide on the problem of the spin-lattice interaction but also because this knowledge is important in the various applications of these particular materials. Divalent thulium has provided the basis for an optically pumped microwave maser⁹ and is also being studied as a means for providing aligned nuclei¹⁰ using optical-pumping techniques. Probably the most important is the application of these materials as sensitive tunable detectors¹¹ for phonons, whose conception was a direct result of these studies.

II. ENERGY LEVELS OF Tm^{2+} ION

The ground configuration of divalent thulium in the cubic hosts CaF_2 , SrF_2 , and BaF_2 is 2F . The spin-orbit coupling splits the 2F into the two states $^2F_{5/2}$ and $^2F_{7/2}$ spaced by about 9000 cm^{-1} with the latter state lowest. Under the influence of a cubic crystalline electric field, the $^2F_{7/2}$ state splits into two doublets $E_{5/2}$ and $E_{1/2}$ and a quartet G with the $E_{5/2}$ state lowest. The ground state is split into four levels under the influence of a magnetic field because of the 100% abundant Tm^{169} isotope which has a nuclear spin $I = \frac{1}{2}$ with a hyperfine coupling of about 1.1 GHz.

A considerable amount of optical and paramagnetic resonance data has been published. The energy levels of Tm^{2+} in CaF_2 were published by Kiss¹² and are shown in Fig. 1 where the Zeeman splittings of the $E_{5/2}$ doublet is about 48 GHz for 10 kG. The energy levels of Tm^{2+} in SrF_2 and BaF_2 are similar and have been measured by Weakliem.¹³ Hayes¹⁴ has reported on the ground-state properties of Tm^{2+} in CaF_2 , while Sabisky and Anderson⁹ have shown that the ground-state properties of Tm^{2+} in SrF_2 and BaF_2 are similar to

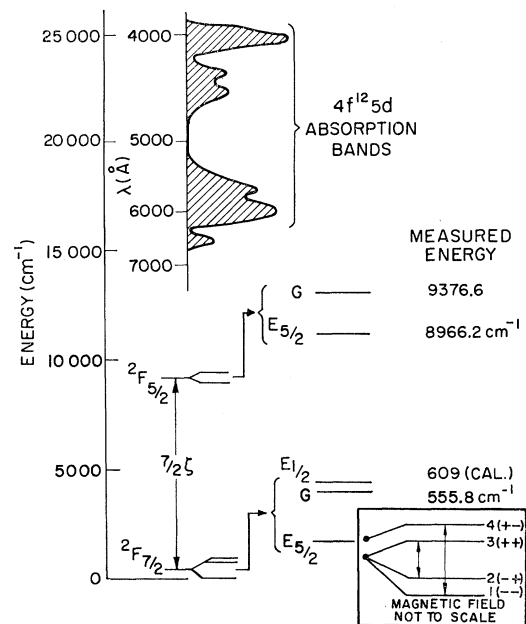


FIG. 1. Energy levels of $CaF_2:Tm^{2+}$.

those of Tm^{2+} in CaF_2 . An interesting feature of the broad absorption bands starting at about 6500 \AA is that they have large circular dichroism.¹⁵

III. EXPERIMENTAL TECHNIQUES

Measurements of the relaxation time were made over a magnetic field range of 1 to 12 kG and a temperature range of 1.2 to 20°K . A measurement technique using optics was employed⁸ which eliminated the need for microwave sources under certain circumstances. A paper discussing this technique in detail is forthcoming and only a brief summary will be given in this paper.

If the paramagnetic ion has broad bands associated with it and if these bands show some magneto-optic effect such as circular dichroism or Faraday rotation, the magneto-optic effect can be used to monitor some properties of the ground state. For an isolated doublet which is the case for Tm^{2+} , it has been shown¹⁵ that the fractional change of the induced circular dichroism (circular dichroism was used entirely in these experiments) is directly proportional to the population difference of the Zeeman levels. The fractional change in the circular dichroism is given by $(\sigma_+ - \sigma_-)/(\sigma_+ + \sigma_-)$, where σ_{\pm} are the absorption coefficients for the two components of circularly polarized light directed along the magnetic field. This change is directly related to the ground-state population difference by the relation-

⁸ There are a number of papers dealing with the dynamic measurement of T_1 by using magneto-optic properties like circular dichroism and Faraday rotation: J. M. Daniels and K. E. Reickhoff, *Can. J. Phys.* **38**, 604 (1960); W. S. C. Chang and J. Q. Burgess, *Appl. Opt.* **1**, 329 (1962); N. V. Karlov, J. Margerie, and V. Merle D'Aubigne, *J. Phys. (Paris)* **24**, 717 (1963); Charles K. Asawa and Robert A. Satten, *Phys. Rev.* **127**, 1542 (1962); Heins Kalbfleisch, *Z. Physik* **181**, 13 (1964); H. Panepucci and L. F. Mollenauer, *Phys. Rev.* **178**, 589 (1969).

⁹ E. S. Sabisky and C. H. Anderson, *IEEE J. Quant. Electron.* **QE-3**, 287 (1967).

¹⁰ L. F. Mollenauer, W. B. Grant, and C. D. Jeffries, *Phys. Rev. Letters* **20**, 488 (1968).

¹¹ C. H. Anderson and E. S. Sabisky, *Phys. Rev. Letters* **18**, 236 (1967); **21**, 987 (1968); *Appl. Phys. Letters* **13**, 214 (1968).

¹² Z. J. Kiss, *Phys. Rev.* **127**, 718 (1962).

¹³ H. A. Weakliem (private communication).

¹⁴ W. Hayes and J. W. Twidell, *J. Chem. Phys.* **35**, 1521 (1961); R. G. Bessent and W. Hayes, *Proc. Roy. Soc. (London)* **A285**, 430 (1965).

¹⁵ C. H. Anderson, H. A. Weakliem, and E. S. Sabisky, *Phys. Rev.* **143**, 223 (1966).

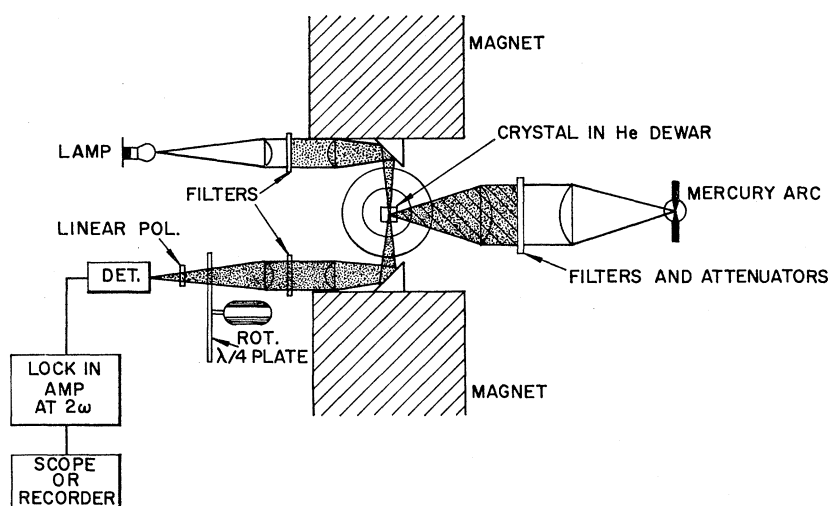


FIG. 2. Experimental arrangement for measurement of T_1 without the use of microwaves.

ship

$$\frac{\sigma_+ - \sigma_-}{\sigma_+ + \sigma_-} = A \frac{n_l - n_u}{n_l + n_u} = A \tanh \frac{h\nu}{2kT}, \quad (1)$$

where A is a constant, ν is the frequency, T is the temperature, and n_l , n_u are the population densities of the two Zeeman levels. To be correct, n_l should be replaced by $n_1 + n_2$ and n_u by $n_3 + n_4$ in Eq. (1) since the ground state of Tm^{2+} has four levels because of its nuclear spin. However, the experiments were performed at frequencies large compared to the hyperfine splitting and therefore the hyperfine effects can be ignored in this case.

The experimental arrangement for measuring T_1 without the use of microwaves is shown in Fig. 2. In this case, a pulsed optical source filtered to match one of the broad absorption bands is used to heat the spins while a low-power, continuous optical source directed along the magnetic field and filtered to match another one of the bands is used to monitor the transient recovery of the spins from their nonequilibrium population distribution. The intensity of the monitor light as is the case with microwaves must be kept low so as not to alter the population distribution. The product of the total absorption coefficient, the thickness of the crystal, and the fractional change in circular dichroism must be less than approximately 0.1 in order for Eq. (1) to be of such a simple form. The low-intensity monitor beam, after having passed through the crystal, passes through a quarter-wave plate rotating at frequency ω , a fixed linear polarizer, and is detected by a photodiode. The output of a photodiode is generally fed into a lock-in detector which is tuned to 2ω for detection of the change in the circular dichroism. For the measurement of long times, the signal was directly fed to a chart recorder. For short times, the transient recovery cycle was averaged over several cycles to improve the signal to noise by a PAR Waveform

Eductor.¹⁶ To measure very fast relaxation times, the rotating quarter-wave plate and the linear polarizer were replaced by a fixed circular polarizer. In this case, only one of the circularly polarized components of the light is incident on the photodiode. It should be emphasized that the experimental arrangement of Fig. 2 can be used to obtain a *continuous* plot of the relative relaxation rate as a function of the magnetic field or frequency as will be shown.

We would like to emphasize that the technique is easy to install and use. For example, the light source that was used is a 6-V tungsten microscope lamp. The helium dewars were round and no special glass was used. The signals were large and it was not necessary to have the light parallel to the direction of the magnetic field. The signal intensity decreases as $\cos\theta$ (θ is the angle between the magnetic field and the propagation direction of the light), and at a convenient angle of 45° the signal is only reduced by 30%.

The relaxation measurements were also made using various combinations of optical and microwave techniques. The population distribution was perturbed at different times using pulsed microwaves, light, heat, and magnetic field and continuous light. The monitor used in general was light where the change in the induced circular dichroism was used to record the transient recovery of the spins to their thermal equilibrium distribution. The combination of light as a monitor with microwaves, heat, or magnetic field to heat the spins has the advantage of eliminating the troublesome cross-talk between the monitor and saturating sources. The temperature-dependent data were obtained using a pulsed microwave source to heat the spins and an optical monitor. Cross checks of the data using the various techniques of spin heating and detection were made to ensure that the data were consistent. In the

¹⁶ Manufactured by Princeton Applied Research Corporation.

temperature-dependent experiments, the crystals were placed in a microwave cavity which contained holes to permit passage of the monitor beam through the crystal. For measurements above 4.2°K, the microwave cavity, a calibrated germanium thermometer, and a heater were placed inside a glass vacuum can. The can was immersed in the liquid helium and contained helium exchange gas to obtain temperature stability and uniformity.

IV. CRYSTALS

The majority of the crystals used in these experiments were grown at RCA Laboratories by H. Temple using a modified gradient freeze technique. The crystals were grown in a helium atmosphere with about 10% HF gas. Crystals from other sources were also measured but were found to be inferior in the low-field region and had relaxation rates which were about an order of magnitude larger near 10 GHz. The divalent state of Tm was obtained by baking the crystals in a metal vapor¹⁷ of the cation. The influence of the fraction of Tm^{3+} converted to Tm^{2+} on the relaxation time of Tm^{2+} is difficult to assess, but it appears that it is of less importance than that of other impurities in the crystals. Trivalent thulium is nonmagnetic. Some measurements were made on crystals where the Tm was reduced by γ irradiation. In these crystals, the relaxation rates were generally two to three orders of magnitude larger than the rates obtained using good crystals at frequencies near 10 GHz. The concentration of Tm varied between 0.001 and 0.05%. The effect of concentration in this range was not significant in influencing the relaxation times in the region of interest (16 GHz and above). It was found that CaF_2 more so than SrF_2 or BaF_2 contained impurities which had an effect on the relaxation time of Tm^{2+} . This is shown in Fig. 3, where a continuous plot is shown of the relative relaxation rate as a function of magnetic field using the experimental

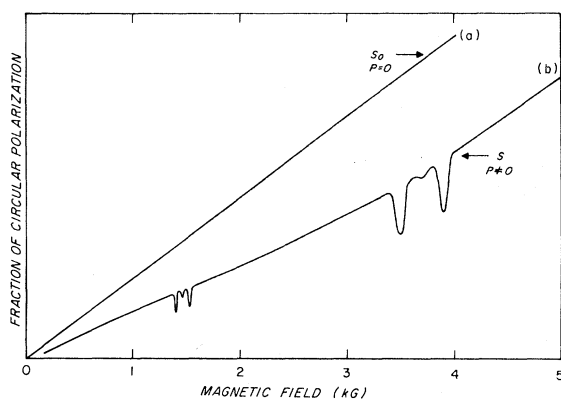


FIG. 3. Continuous measurement of the relative relaxation rate for 0.02% Tm in CaF_2 at 1.4°K showing cross relaxation with Ho^{2+} .

¹⁷ Z. J. Kiss and P. N. Yocom, *J. Chem. Phys.* **41**, 1511 (1964).

arrangement of Fig. 2. In the figure, the curve S_0 , $P=0$, is a plot of the change in the circular dichroism in the absence of spin heating light. The curve S is a plot of the change in the circular dichroism for a fixed amount of pumping light $P \neq 0$. The curve S is related to S_0 by the relationship $S = S_0/1 + pT_1$ or $T_1^{-1}/p = S/(S_0 - S)$. In this manner, continuous plots as shown in Fig. 3 of the relative relaxation rate can be made and any sharp cross-relaxation peaks detected. The data shown in the figure were obtained using a so-called pure 0.02% Tm doped CaF_2 crystal. The peaks have been identified with Ho^{2+} and will be discussed in another paper. By mass spectrographic analysis and by electron spin resonance, the amount of Ho present in these crystals was measured to be 0.06 ppm. For crystals which were intentionally doped with both Tm and smaller amounts of Ho, the magnetic-field dependence of the relaxation rate displayed by this technique clearly shows a large number of overlapping lines which are very difficult to interpret. The importance of very small amounts of impurities in these crystals on the relaxation rate of the weakly coupled Tm^{2+} ion is evident. This technique was used to sort out poor crystals or crystals in which the relaxation rate was abnormal. In many of these poor crystals, it was found that the relaxation rate was essentially independent of frequency, sometimes over the entire field range of 1 to 6 kG, as shown in several later figures.

V. HYPERFINE EFFECTS

The 100% abundant Tm^{169} isotope has a nuclear spin $I = \frac{1}{2}$ and adds some minor difficulties to the interpretation of the data. Baker and Ford¹⁸ have given a theoretical treatment of the effect of the hyperfine term on the one-phonon process. To first order, the existence of the Raman and Orbach processes does not require mixing by the magnetic field, and no dependence on hyperfine terms is expected.

Divalent thulium is a Kramer's ion and the essential point of a hyperfine term is that the perturbation which admixes the ground doublet with higher states is for $H \parallel Z$ given by

$$3\mathcal{C} = (\Delta\beta H + aI_z)J_z + \frac{1}{2}a(J_+I_- + J_-I_+) \quad (2)$$

instead of the perturbation $\Delta\beta H J_z$ for isotopes with $I=0$. A is the Landé g factor and a is the free-ion hyperfine-interaction constant. The new feature is that the ground doublet is now a multilevel system and there are several types of transitions to be considered.

In this high-field study, we are only interested in the allowed hyperfine transitions and therefore need only concern ourselves with the first term in the above equation. This term causes admixtures into the ground doublet of excited states with the same nuclear quantum

¹⁸ J. M. Baker and N. C. Ford, Jr., *Phys. Rev.* **136**, A1692 (1964); G. H. Larson and C. D. Jeffries, *ibid.* **145**, 311 (1966).

state m_I producing relaxation of the ground-state transitions in which $\Delta M_J = \pm 1$, $\Delta m_I = 0$. Under this high-field condition, the direct process¹ may be written as

$$T_1^{-1} = B \frac{\nu^3}{\Delta_i^2} \left(H + \frac{A}{g\beta} m_I \right)^2 \coth \left(\frac{h\nu}{2kT} \right), \quad (3)$$

where ν is the frequency, Δ_i is the energy separation of excited states. The hyperfine constant a was converted to the constant A which is based on the common spin-Hamiltonian formulation. Also, for magnetic fields when $g\beta H \gg Am_I$ (above 2 kG for Tm^{2+}),

$$h\nu = g\beta [H + (A/g\beta)m_I].$$

Thus, for experiments performed at a constant microwave frequency, the relaxation rate is independent of m_I and should be the same as the rate for isotopes with $I=0$, namely,

$$T_1^{-1} = K \frac{\nu^5}{\Delta_i^2} \coth \left(\frac{h\nu}{2kT} \right). \quad (4)$$

This was verified a number of times and was used as one test for the selection of crystals without cross-relaxation. In the early stages of the study, it was not uncommon for the relaxation rates of the two allowed hyperfine lines to differ by as much as 50%. The relaxation rates for the transitions defined by $\Delta M_J = \pm 1$, $\Delta m_I = \mp 1$ were not examined in any detail. These transitions are not expected to measurably perturb the relaxation of the $\Delta m_I = 0$ transitions. In the region of interest in this study, the relaxation rates of the weakly coupled transitions are expected to be less by the ratio $(A/\Delta\beta H)^2$, which is equal to 1/40 for magnetic fields of 4 kG, which is the lower-field range of the experiment.

The majority of the measurements presented in this paper were obtained using an optical detection scheme which does not separate the two allowed hyperfine transitions. This under certain conditions introduces some uncertainty in the data. As seen by Eq. (3), two decay rates should be present at a fixed magnetic field for Tm^{2+} since $m_I = \pm \frac{1}{2}$. Indeed, for fields below 2 kG, the decay curves were not single exponentials. However, at fields above 3 kG, the influence of the hyperfine term is small and the two decay rates become indistinguishable within the accuracy of the experiment. The hyperfine term introduces an uncertainty of about $\pm 10\%$ at 3 kG which decreases with the square of the field. In summary, the data used to evaluate the one-phonon process were taken above 3 kG and the influence of the hyperfine field can be neglected. Equation (4) for isotopes of $I=0$ was used to compare the data.

VI. EXPERIMENTAL RESULTS

Using the method presented in this paper for measuring the spin-lattice relaxation time, a large number

of crystals from different sources, varying thulium concentration, and different reduction techniques for obtaining the divalent state of thulium were examined. The selected data are intended to show unambiguous verification of the one-phonon process, angular dependence of the one-phonon process, and the importance of frequency-dependent over temperature-dependent measurements for identification of the single-phonon process.

A. Tm^{2+} in SrF_2

Figure 4 shows the experimental results of the field dependence of T_1 at 1.38°K. In order not to be overwhelmed with data, the continuous measurements which were taken of the field dependence of T_1 are not shown except when specifically noted and only the data obtained at fixed magnetic fields are plotted in all the figures. Above a certain magnetic field which is a function of the crystal the expected H^4 dependence of the relaxation rate for the one-phonon process is clearly observed. The data in the high-field region show that the relaxation rate is independent of Tm concentration and crystal orientation. Notice the large disparity of the data between crystals at low magnetic fields and the agreement at high magnetic fields where the one-phonon process is dominant. In the low-field region, the relaxation rate is dominated by processes other than the one-phonon process. The rate at fields of 1–2 kG

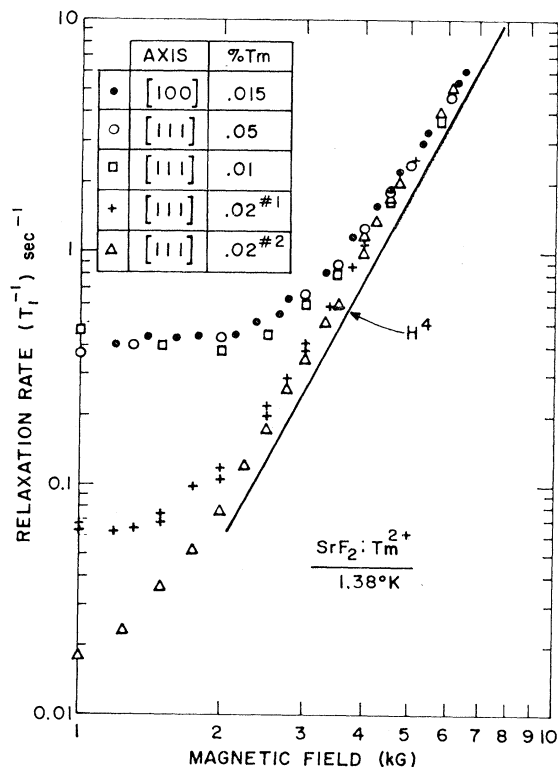


FIG. 4. Field dependence of relaxation rate for Tm^{2+} in SrF_2 .

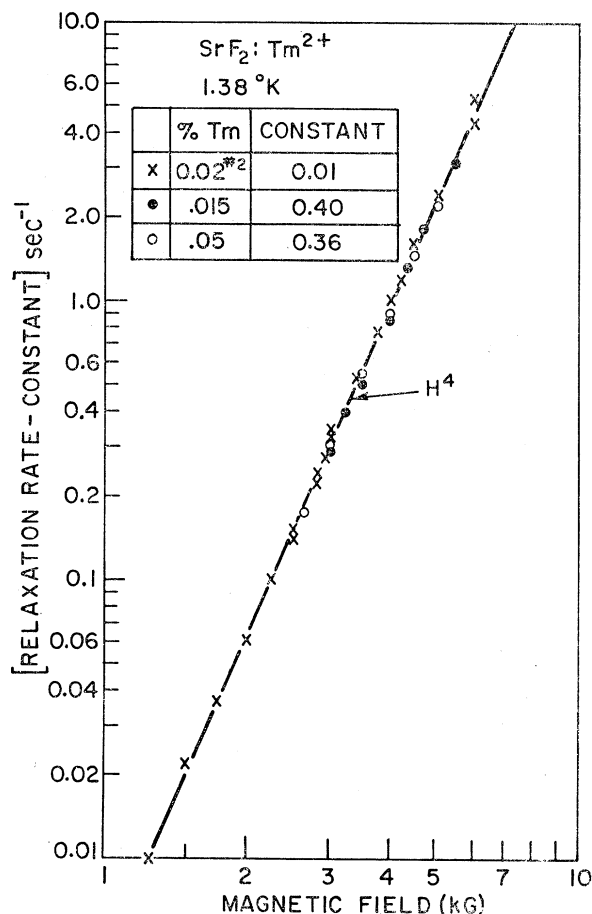


FIG. 5. Field dependence of relaxation rate minus a constant value for Tm^{2+} in SrF_2 .

can vary by more than three orders of magnitude depending on the crystal. In good crystals, relaxation times as long as 70 sec have been measured while some crystals had times as short as msec. The data shown in Fig. 4 are indicative of that of Tm^{2+} in CaF_2 and BaF_2 . That is, the relaxation rate varies as H^4 at high magnetic fields and reaches some minimum value somewhere between 0.5 and 2 kG and begins to increase again as the field is further reduced. The field-independent region in poor crystals often extends over the entire magnetic field range of the experiment.

This paper is mainly concerned with a study of the one-phonon process, and the anomalous results in the low-field region need not concern us. However, since the anomaly appears to be field independent, there is some justification for subtracting this constant from the measured value. The result is shown in Fig. 5, where the H^4 dependence over an extended field range is obtained. Similar plots of Tm^{2+} in CaF_2 and BaF_2 yield similar results. This is only an interesting observation and was not used to interpret the one-phonon process.

The anomalous field-independent region has another interesting feature. The relaxation rate measured in this region was found to be proportional to temperature and on this basis can be misinterpreted as the one-phonon process. It is seen that identification of the one-phonon process using only temperature dependence is not sufficient and probably is responsible for the majority of the discrepancies on relaxation times which appear in the literature.

To make the temperature-dependent measurements given in this paper, the operating frequency was chosen by first making field-dependent measurements on the particular crystal. In some crystals in addition to the anomaly at low magnetic fields, sharp cross-relaxation peaks appear as shown in Fig. 3 and these regions must also be excluded as operating points. Using the 0.02% sample whose frequency dependence is shown in Fig. 4, measurements of the temperature dependence were made at K-band frequency (~ 4 kG). The results are given in Fig. 6. The rate is proportional to temperature up to about 4°K, where the Raman process begins to manifest itself with its characteristic T^9 temperature dependence. The largest uncertainties in fitting the data occurred in the region where both relaxation processes are comparable. However, the data were fitted to within the experimental accuracy and more accurate data need to be taken to check on the relaxation in this region. A number of experiments were done to measure the angular dependence of the one-phonon

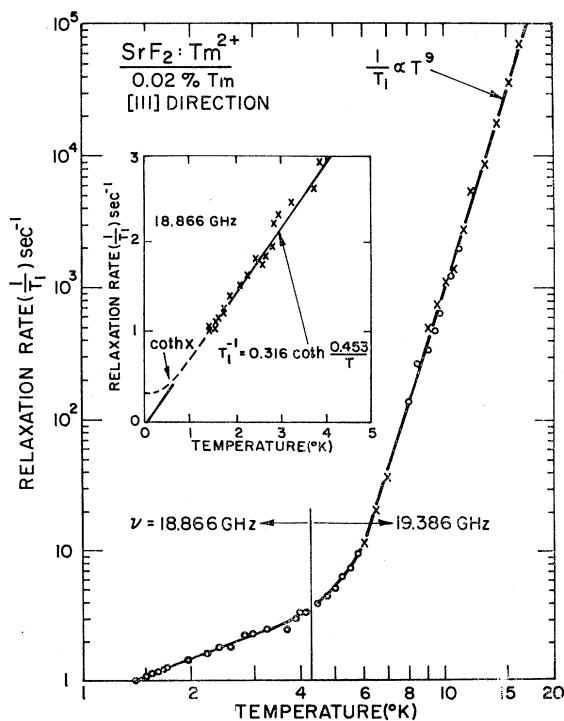


FIG. 6. Temperature dependence of relaxation rate for Tm^{2+} in SrF_2 .

process at a fixed microwave frequency. The relaxation rate was found to be independent of crystal orientation to within $\pm 5\%$. The temperature-dependent data taken at 18.866 GHz for the linear region can be fitted by the equation

$$T_1^{-1} = (0.316 \pm 0.02) \coth(0.453/T) \text{ sec}^{-1}. \quad (5)$$

Putting $h\nu = g\beta H$ and taking the first term in the expansion of the coth function, Eq. (5) can be written as

$$T_1^{-1} = (30 \pm 2) \times 10^{-4} H^4 T, \quad (6)$$

where T is in $^\circ\text{K}$ and H is in kG. The results of the frequency-dependent measurements taken at 1.38 $^\circ\text{K}$ are fitted by

$$T_1^{-1} = (29 \pm 3) \times 10^{-4} H^4 T. \quad (7)$$

The agreement between the two methods is within experimental error. As discussed in the section on hyperfine effects, the magnetic field in the above equations is the applied field which can be satisfactorily used to the accuracy of the experiment above 3 kG.

B. Tm^{2+} in CaF_2

The frequency- or field-dependent measurements for two crystals are shown in Fig. 7. The data are similar

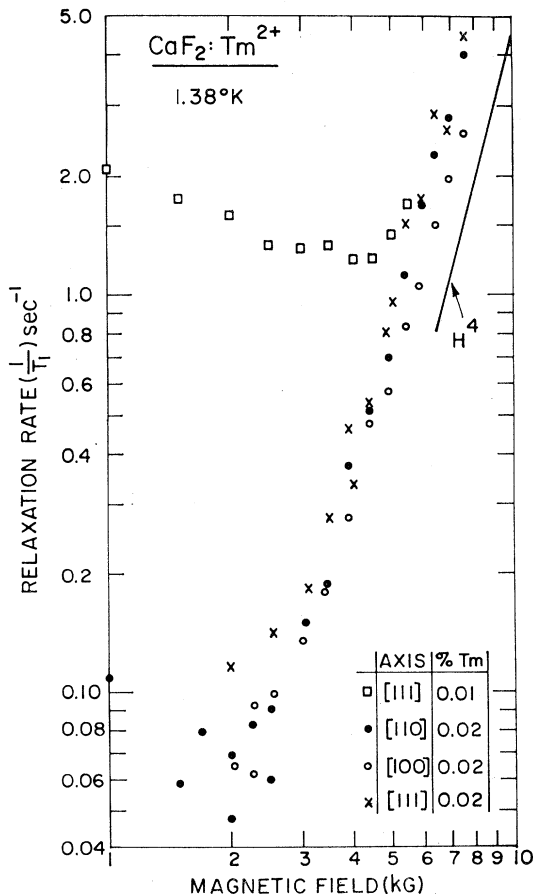


FIG. 7. Field dependence of relaxation rate for Tm^{2+} in CaF_2 .

to that of Tm^{2+} in SrF_2 . An H^4 dependence is only observed above a certain value of magnetic field while the data at low fields reflect relaxation mechanisms other than the direct process. One large difference is that an angular dependence is clearly observed. More accurate data of the angular dependence were obtained by making measurements at a fixed frequency (27 GHz) and rotating the magnetic field with respect to the crystal. In this case, a pulsed microwave source was used to saturate the spins. The data points are shown in Fig. 8, where the curve drawn through the points was obtained using an expression derived in the Appendix. Figure 9 shows additional data of the field dependence of the relaxation rate. These data are shown separately since the measurements were obtained using a pulsed heater to change the equilibrium distribution of the ground-state population whereas all the other frequency-dependent measurements were

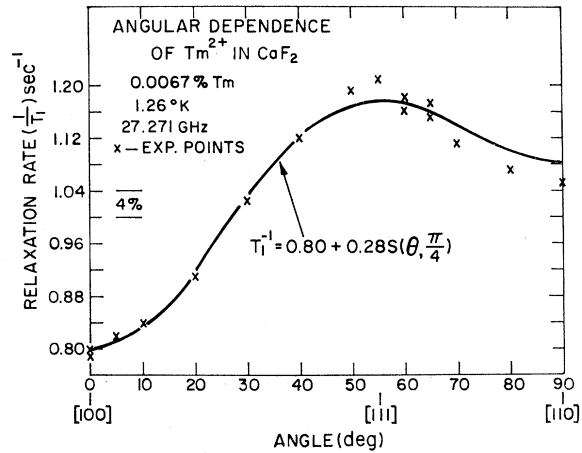


FIG. 8. Angular dependence of relaxation rate for Tm^{2+} in CaF_2 .

done using light or magnetic field to change the population distribution from its equilibrium value. The heater consisted of a short length of high-resistance wire which was wrapped around part of the crystal. This heater-crystal combination had a thermal time constant of a few milliseconds while the spin-lattice relaxation time at the highest field in the experiment was 51 msec. By making heaters which can be pulsed in the μsec region, this method of obtaining the frequency dependence of the relaxation rate can be employed for a large number of ions.

As was done for SrF_2 , the experiments on the temperature dependence were performed outside any anomalous magnetic field regions. The results are shown in Fig. 10, where the rate is proportional to temperature to about 5 $^\circ\text{K}$ and the characteristic T^9 dependence is observed at the higher temperatures. The temperature-dependent measurements for the direct region for the [100] direction can be fitted by the equation

$$T_1^{-1} = (5.9 \pm 0.5) \times 10^{-4} H^4 T. \quad (8)$$

The frequency-dependent data obtained using an optical source to heat the spins and shown in Fig. 7 for the [100] direction are described by

$$T_1^{-1} = (5.6 \pm 0.5) \times 10^{-4} H^4 T. \quad (9)$$

The data obtained using a heater as the pump and shown in Fig. 9 are described by

$$T_1^{-1} = (6.9 \pm 0.5) \times 10^{-5} H^5 \coth \frac{g\beta H}{2kT}. \quad (10)$$

This equation fits the experimental results from 5 to 12 kG. The agreement between the three methods is as was the case for SrF_2 within the experimental accuracy.

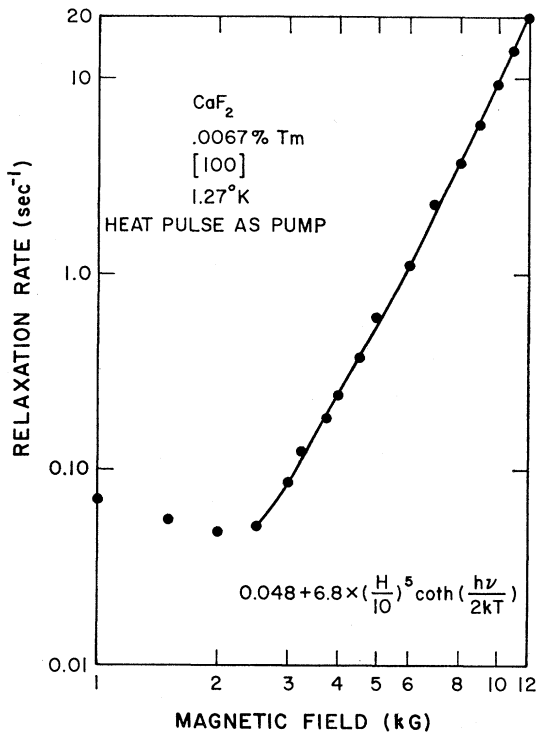


FIG. 9. Measured field dependence of relaxation rate for Tm^{2+} in CaF_2 using a heater to change the population distribution from equilibrium.

As was discussed previously, temperature-dependent measurements of the relaxation rate near 2 kG (~ 10 GHz) were found to be proportional to temperature and can be erroneously interpreted as the one-phonon process for the isolated divalent thulium ion. Huang¹⁹ made temperature-dependent measurements near 10 GHz of Tm^{2+} in CaF_2 and obtained a value of $T_1^{-1} = 13 T$ for the one-phonon process. However, using the results from this paper, the relaxation rate near 10 GHz for the one-phonon process is $T_1^{-1} = 0.01 T$, a disagree-

¹⁹ Chao-Yuan Huang, Phys. Rev. **139**, A241 (1965); **169**, 470 (1968).

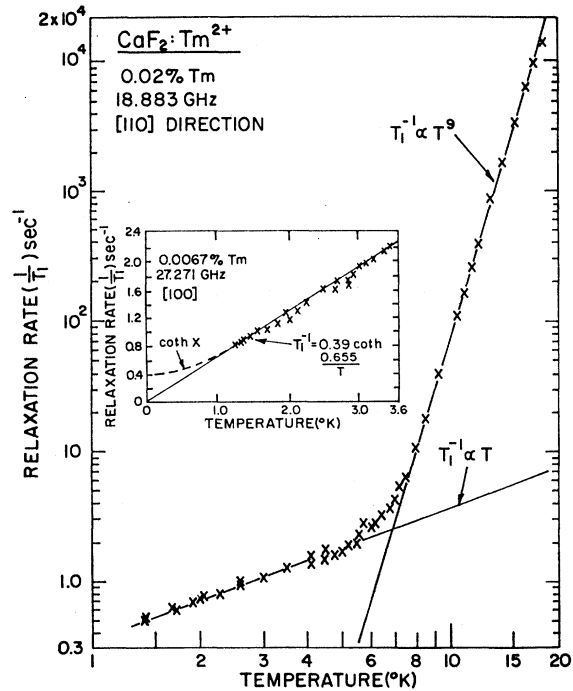


FIG. 10. Temperature dependence of the relaxation rate for Tm^{2+} in CaF_2 .

ment between the two values of 3 orders of magnitude. Clearly the use of only temperature-dependent measurements is questionable, particularly in cases when there is weak coupling between ion and lattice.

C. Tm^{2+} in BaF_2

Figure 11 shows the field-dependent measurements for only one crystal so that the angular dependence can be made apparent. As with Tm^{2+} in CaF_2 and SrF_2 , the characteristic H^4 dependence is only observed at the higher magnetic fields. More accurate data of the angular dependence was obtained by operating at a fixed frequency and rotating the magnetic field. The angular dependence is similar to that found for Tm^{2+} in CaF_2 (Fig. 8), but for Tm^{2+} in BaF_2 the maximum rate occurs along the [100] and not the [111] direction.

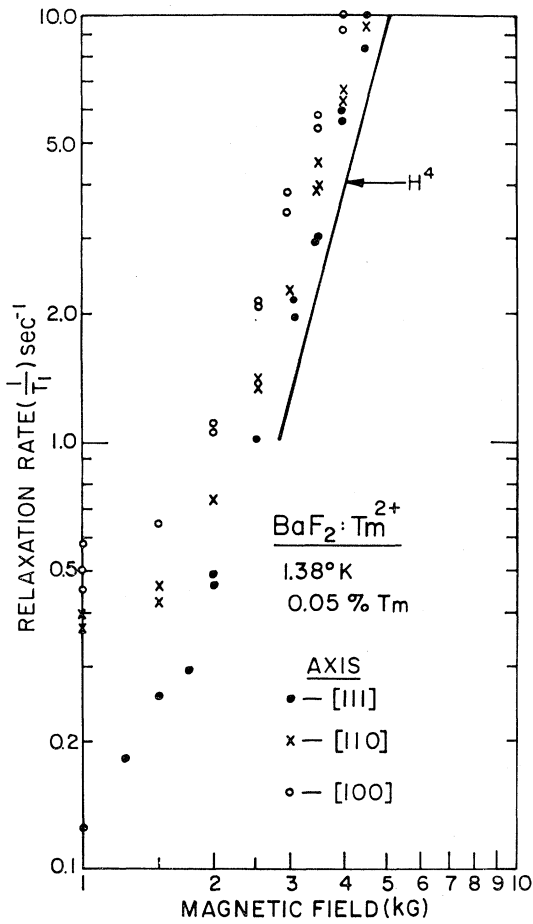
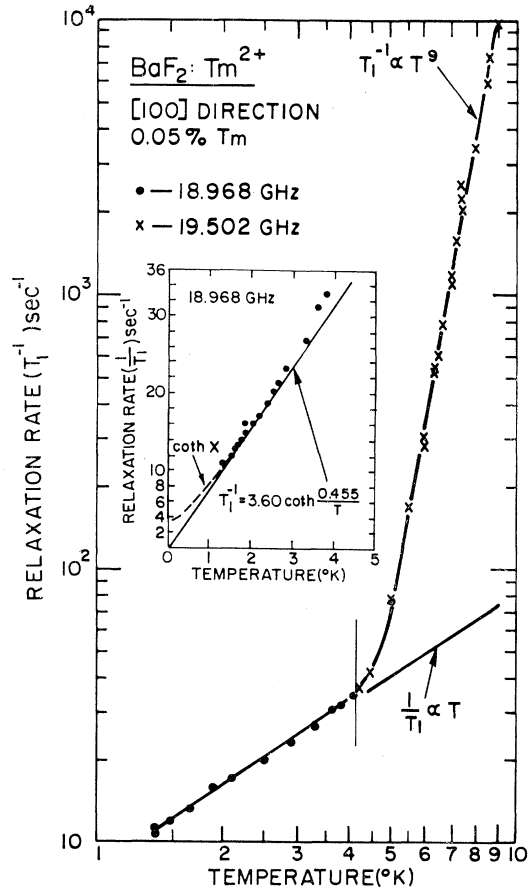
The temperature-dependent results are shown in Fig. 12, where, as before, the one-phonon and two-phonon processes are obtained. The temperature-dependent data for the direct process along the [100] direction can be described by

$$T_1^{-1} = (324 \pm 15) \times 10^{-4} H^4 T. \quad (11)$$

The frequency- or field-dependent data for the [100] direction are fitted by

$$T_1^{-1} = (300 \pm 30) \times 10^{-4} H^4 T, \quad (12)$$

where again the agreement between the two methods is within the experimental accuracy. A summary of the experimental data is given in Table I.

FIG. 11. Field dependence of relaxation rate for Tm^{2+} in BaF_2 .FIG. 12. Temperature dependence of relaxation rate for Tm^{2+} in BaF_2 .

VII. COMPARISON WITH THEORY

A. One-Phonon Process

The calculation of the spin-lattice relaxation time is based on the unpublished work of Inoue.²⁰ The model used by Inoue is that employed by Van Vleck,³ that is, a simple point-charge model and the Debye spectrum to describe the lattice oscillators. The spin-lattice

relaxation rate W for the direct process is defined by

$$W = 1/T_1 = \omega_{a \rightarrow b} + \omega_{b \rightarrow a}, \quad (13)$$

where $\omega_{b \rightarrow a}$ is the transition probability per unit of time that the spin flips from the upper state $|b\rangle$ to the lower state $|a\rangle$ by emitting a phonon of energy equal to the energy separation of the doublet. The usual expression

TABLE I. Experimental results for the relaxation rate of Tm^{2+} in CaF_2 , SrF_2 , and BaF_2 . Here, H is in kG, T in $^{\circ}K$; $S(\theta, \frac{1}{4}\pi) = \sin^2 2\theta + \sin^4 \theta \sin^2 [2(\frac{1}{4}\pi)]$; $[111]/[100]$ refers to (relaxation rate along $[111]$)/(relaxation rate along $[100]$).

Host	[100] Direct process rate (sec^{-1})	Direct process angular dependence rate (sec^{-1})	Raman process rate (sec^{-1})
CaF_2	$(6.8 \pm 0.5) \times (H/10)^5 \coth(h\nu/2kT)$	$W = 0.80 + 0.28 S(\theta, \frac{1}{4}\pi)$ for $\nu = 27.27$ GHz, $T = 1.26^{\circ}K$ $[111]/[100] = 1.51$ $[110]/[100] = 1.31$	$(76 \pm 7) \times (T/10)^9$
SrF_2	$(34.6 \pm 2) \times (H/10)^5 \coth(h\nu/2kT)$	no angular dependence to 5%	$(1000 \pm 100) \times (T/10)^9$
BaF_2	$(374 \pm 15) \times (H/10)^5 \coth(h\nu/2kT)$	$W = 11 - 4.0 S(\theta, \frac{1}{4}\pi)$ for $\nu = 19.02$ GHz, $T = 1.38^{\circ}K$ $[111]/[100] = 0.50$ $[110]/[100] = 0.64$	$(26\,000 \pm 3000) \times (T/10)^9$

²⁰ Michiko Inoue, thesis, Harvard University, 1963 (unpublished).

for the transition probability is

$$\omega_{b \rightarrow a} = \frac{2\pi}{\hbar} |\langle a | V_{OL} | b \rangle|^2 \rho(E),$$

where $\rho(E)$ is the density of final states and V_{OL} is the orbit-lattice interaction. To define V_{OL} , a Taylor-series expansion is made of the crystal field at the impurity site in terms of either the normal coordinates or the ordinary ionic displacements of the XY_8 cluster. The first term of the expansion represents the local static potential, and the second term which is linear in the lattice displacements is the orbit-lattice interaction for the direct process.

From the symmetry of the XY_8 complex, the number of terms in the expansion for V_{OL} can be reduced from 27 normal coordinates to eight. We are left with two terms which transform like E_g and six terms which transform like T_{2g} . In addition, applying the conditions of orthogonality and inversion symmetry for f electrons, spherical harmonics other than those of the second, fourth, and sixth order are eliminated. It is further assumed that the wavelength of the lattice vibrations that are of interest is long compared with the size of the cluster. This assumption is a very good approximation for all present measurements of T_1 and is responsible for the elimination of one of the repeated T_{2g} representations. This means we need only consider one E_g and one T_{2g} representation. The orbit-lattice interaction can be written more explicitly as

$$V_{OL} = \sum_{n=2,4,6} \sum_{m=0,2} A(nE_g) B(nE_g m) Q(E_g m) + \sum_{n=2,4,6} \sum_{m=\pm 1,2} A(nT_{2g}) B(nT_{2g} m) Q(T_{2g} m), \quad (14)$$

where $B(n\Gamma m)$ and $Q(\Gamma m)$ are appropriate combinations of spherical harmonics and ionic displacements, respectively. The dynamic crystal field coefficients $A(n\Gamma)$ are associated with a particular irreducible representation and an orbital quantum number n , where n is the order of the spherical harmonics. The calculation involving the Q 's proceeds by expanding the Q 's in terms of the thermal vibrations of the entire crystal using the Debye model.

To make the calculation tractable, a statistical average is taken over the vibrational states and a directional average is taken assuming the lattice is elastically isotropic. In general, the crystals are not elastically isotropic as is the case for CaF_2 and SrF_2 . However, BaF_2 is elastically isotropic. This is probably not too important an assumption for predicting the magnitude of T_1 but may influence the angular dependence.

After performing the mathematical operations on the vibrational part of the orbit-lattice interaction, the spin-lattice relaxation rate W as given by Inoue²⁰

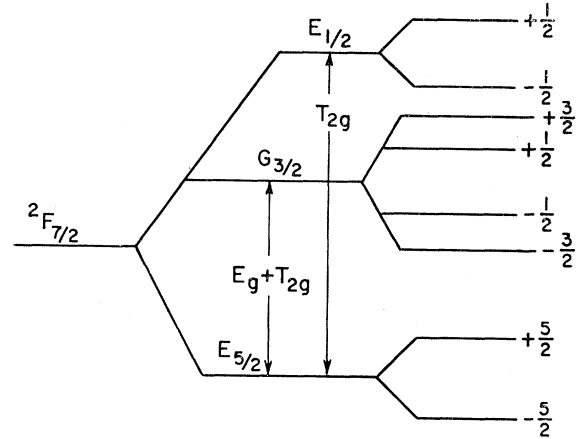


FIG. 13. Splitting of the ${}^2F_{7/2}$ multiplet of Tm^{2+} in a cubic crystalline field and a magnetic field.

is found to be

$$W = \frac{1}{T_1} = \frac{32\pi^3 \nu^3}{15\hbar \rho v_i^5} \coth\left(\frac{\hbar\nu}{2kT}\right) \sum_j |\langle a | V_j | b \rangle|^2, \quad (15)$$

where V_j are the electronic operators of the V_{OL} , v_i is the transverse sound velocity, and ν is the frequency. Since the longitudinal sound velocity is generally about twice the transverse sound velocity and they both enter the equations in the fifth power, the term containing the longitudinal velocity was dropped. Since divalent thulium is a Kramers ion, relaxation can only occur through the admixture of excited states into the ground state by the applied magnetic field. The above equation under the conditions $\hbar\nu = g\beta H$, $\hbar\nu \ll 2kT$, and H parallel to the $[100]$ direction becomes

$$W = \left(\frac{256\pi^3 k\beta^4}{15\hbar^4}\right) \left(\frac{\Lambda^2 g^2 H^4 T}{v_i^5 \rho}\right) \times \sum_j \left| \sum_i \frac{\langle b | J_z | p_i \rangle \langle p_i | V_j | a \rangle}{\Delta_{p_i}} \right|^2, \quad (16)$$

where ρ is the density, Λ is the Landé g factor, $|p_i\rangle$ are the state vectors of the excited states, and Δ_{p_i} is the energy separation of the excited states from the ground state. For Tm^{2+} in CaF_2 , SrF_2 , and BaF_2 , $g=3.45$ and $\Lambda=8/7$. Therefore, the parameters which change with the fluoride lattice are the density, the transverse sound velocity, the position of the excited states, and the matrix element which under this model is a function of the lattice spacing. The excited states of interest are shown in Fig. 13. The other excited states are at least 9000 cm^{-1} away and are neglected. To first order, a magnetic field does not admix the two doublets and so the $E_{1/2}$ state does not contribute to the relaxation of the one-phonon process. They do, however, contribute to the Raman relaxation process. The wave functions for the three states of Tm^{2+} are well defined and are

TABLE II. Some parameters of Tm^{2+} in the cubic hosts.

Host	Position of $G_{3/2}$ states ^a (cm ⁻¹)	Density ^b (g/cm ³)	Transverse sound velocity along cube axis v_t (cm/sec)	$\frac{K}{\text{cm}^2/\text{kG}^4 \text{ } ^\circ\text{K sec}}$
CaF ₂	556	3.18	3.34×10^5 ^c	3.13×10^{-9}
SrF ₂	474	4.24	2.80×10^5 ^d	7.9×10^{-9}
BaF ₂	405	4.89	2.27×10^5 ^e	27.4×10^{-9}

^a These data were kindly supplied by H. A. Weakliem.

^b *Handbook of Chemistry and Physics* (Chemical Rubber Publishing Co., Cleveland, Ohio, 1967-68).

^c D. R. Huffman and M. H. Norwood, Phys. Rev. 117, 709 (1960).

^d D. Gerlick, Phys. Rev. 136, A1366 (1964).

^e D. Gerlick, Phys. Rev. 135, A1331 (1964).

given in a number of papers.²¹ Using these wave functions and the coupling coefficients given by Polo²² for the E_g and T_{2g} representations, it is seen that the vibrations of the E_g representation do not contribute to the relaxation along the [100] direction. Thus, in the calculation of the direct process, we are left with a single excited state, $G_{3/2}$, and one type of vibration, T_{2g} .

The magnitude of the matrix element containing the operator J_z is $\sqrt{3}$. The relaxation rate along the [100] direction now becomes

$$W = 2KH^4T|M|^2, \quad (17)$$

where T is temperature in $^\circ\text{K}$, H is the magnetic field in kG, and K is given in Table II and is different for the three hosts because of differences in density, sound velocity, and position of the excited state, $G_{3/2}$.

Based on the point-charge model for the CaF₂ lattice, the square of the magnitude of the matrix element of the orbit-lattice interaction is given by

$$|M|^2 = 3|422 - 19.2 + 3.1|^2 = 4.9 \times 10^5 \text{ cm}^{-2}, \quad (18)$$

where inside the magnitude sign the terms are due to the second-, fourth-, and sixth-order terms of the orbit-lattice interaction, respectively. The mean radii of Tm^{2+} calculated by Freeman and Watson²³ were

TABLE III. Calculated and experimental values of the relaxation rate and $|M|$ along the [100] direction. Local vibrations of T_{2g} symmetry are the only ones effective. Here $|M| = A_{T_2} \langle G_{3/2}, +\frac{3}{2} | \times O_2^{+1} | E_{5/2}, +\frac{5}{2} \rangle = A_{T_2} 2\sqrt{3}$; $A_{T_2} \propto \langle r^2 \rangle / R^3 \langle J_{\parallel} | J \rangle$; $\langle J_{\parallel} | \alpha | J \rangle = 2/63$.

Host	Relaxation-rate coefficient ^a (sec ⁻¹)		$ M $ (cm ⁻¹)	
	Experiment	Theory	Experiment	Theory
CaF ₂	5.9	33	308	730
SrF ₂	30	60	436	615
BaF ₂	324	137	770	500

^a Coefficient of $(H/10)^4 T$, where H is in kG, and T is in $^\circ\text{K}$.

²¹ R. Pappalardo, J. Chem. Phys. 34, 1380 (1961); K. R. Lea, M. J. M. Leask, and W. P. Wolf, J. Chem. Phys. Solids 23, 1381 (1962).

²² S. R. Polo, Air Force Cambridge Research Laboratory Report No. AFCRL-555(II) (unpublished), obtainable from U. S. Department of Commerce, Office of Technical Services, Washington, D. C.; RCA Laboratories Report No. 1911 (unpublished).

²³ A. J. Freeman and R. E. Watson, in *Magnetism*, edited by G. T. Rado and H. Suhl (Academic Press Inc., New York, 1966), Vol. II A.

used. There is a slight difference if the radii of $\langle r^4 \rangle$ and $\langle r^6 \rangle$ derived by Bleaney²⁴ are used. The second-order terms clearly dominate and to within the confidence of the calculation the fourth- and sixth-order terms in the orbit-lattice interaction can be neglected. This also means that only two of the six dynamic crystal field coefficients defined by Eq. (14) can be experimentally determined using spin-lattice relaxation measurements. A comparison between the calculated (using only second-order terms) and experimental values of the relaxation rate and the matrix element of the orbit-lattice interaction is given in Table III. In general, the agreement between theory and experiment is surprisingly good for this type of calculation. Huang's¹⁹ calculation of the relaxation rate for Tm^{2+} in CaF₂ is a factor of 3 below that given in Table III. The discrepancy between the two calculations has not been accounted for.

Note the point-charge model does not explain the variation of T_1 between hosts. The experimental values of $|M|$ are increasing while the calculated values are expected to decrease because of an increasing lattice constant as one goes from CaF₂ to BaF₂. The static crystal field parameters as determined from optical measurements for Tm^{2+} (that is, the fourth- and sixth-order terms) were experimentally¹³ found to decrease but not as rapidly as expected from the point-charge model. Also, the magnitude of the static coefficients of the fourth- and sixth-order terms for CaF₂ are about 4-5 times less than those calculated using the point-charge model.

A calculation of the expected angular dependence of the relaxation rate due to the mixing of the ground doublet with an excited state is given in the Appendix. The results can be written as

$$W = W_{T_{2g}} + [W_{E_g} - \frac{1}{2}W_{T_{2g}}]S(\theta, \phi), \quad (19)$$

where $W_{T_{2g}}$ and W_{E_g} are the relaxation rates along the [100] and [110] directions for T_{2g} - and E_g -type local vibrations, respectively, and $S(\theta, \phi) = \sin^2 2\theta + \sin^4 \theta \times \sin^2 2\phi$. For the [100] direction, $S(\theta, \phi) = 0$ and $W = W_{T_{2g}}$. The experimental data of the angular dependence of Tm^{2+} in CaF₂ and BaF₂ can be fitted to within experimental accuracy as can be seen from Fig. 8. The absence of any angular dependence for Tm^{2+} in SrF₂ can be explained by the above equation if $W_{E_g} = \frac{1}{2}W_{T_{2g}}$.

Thus, using Eq. (19), the relaxation rate due to E_g -type vibrations can be separated out from the total relaxation rate. For the [110] direction, $S(\theta, \phi) = 1$ and $W_{E_g} = W - \frac{1}{2}W_{T_{2g}}$. The second-order term again dominates the calculation if the $\langle r^n \rangle$ values of Freeman and Watson are used. If Bleaney's values for $\langle r^n \rangle$ are used, the fourth-order term differs by only 4 from the second-order term. A comparison between theory using only the second-order term and experiment is given in Table IV. The agreement is again surprisingly good.

²⁴ B. Bleaney, Proc. Roy. Soc. (London) 227, 289 (1964).

TABLE IV. Comparison between theory and experiment for the matrix element $|M|$ for modes of E_g symmetry along the [110] direction. Here, $|M| = A_E |\langle G_{3/2} + \frac{1}{2} | O_2^{2+} | E_{5/2} + \frac{1}{2} \rangle| = A_E 3$.

Host	Matrix element $ M $ (cm^{-1})	
	Experiment	Theory
CaF ₂	450	477
SrF ₂	500	399
BaF ₂	475	327

Note that in this case the experimental value of the matrix element of the orbit-lattice interaction is essentially independent of the hosts.

B. Raman Process

The two-phonon process will not be discussed in detail. In this case, all phonons within the Debye limit can interact with the spin system. For Kramer's ions for temperatures below about 0.1 Debye temperature, the relaxation rate is expected to vary as T^9 and for purposes of this paper can be written as

$$T_1^{-1} = \frac{D}{\rho^2 v_t^{10} \Delta^4} |M|^2 T^9,$$

where D is a constant for Tm^{2+} , and Δ is the position of the excited states. The matrix element M is defined by $|\sum_{jk} \langle a | V_j | p \rangle \langle p | V_k | b \rangle|$. The data in Figs. 6, 10, and 12 above about 5°K identify the Raman process. To calculate the Raman process, the presence of both the $G_{3/2}$ and $E_{1/2}$ states must be taken into account. As shown in Fig. 13, matrix elements are now allowed between the $E_{5/2}$ and $E_{1/2}$ states due to vibrations of T_{2g} symmetry. Theory and experiment for all the three hosts agree to within an order of magnitude, which is about as good as one expects. The values for Tm^{2+} in CaF₂ are in close agreement with the value obtained by Huang.¹⁹ Since second-order terms dominate the calculations, $|M|^2$ is expected to vary inversely with R^{12} , where R is the lattice constant. Table V gives the normalized values of $|M|^2$ as obtained from experiment and as expected from theory. Note the same variation as found for the one-phonon process for relaxation due to vibrations of T_{2g} symmetry.

VIII. SUMMARY

The observed fourth-power dependence on magnetic field in combination with the linear temperature de-

TABLE V. Comparison between theory and experiment of the relative values of $|M|^2$ for the Raman process.

Host	Experiment	Theory
	$ M ^2$	$ M ^2 \propto 1/R^{12}$
CaF ₂	1	1
SrF ₂	2.2	$\frac{1}{2}$
BaF ₂	4.85	1/4.4

pendence of the relaxation rate is strong confirmation of Van Vleck's theory of the one-phonon process for Tm^{2+} . The agreement between the experimental results and theory using a point-charge and Debye models for both the one- and two-phonon processes is good. For the one-phonon process, the matrix element for the orbit-lattice interaction differed by at most a factor of 2.5 between theory and experiment. The calculations showed that the relaxation arises from the second-order terms ($L=2$) in the orbit-lattice interaction. These terms are absent in the cubic static crystalline field and are slowly converging with respect to the distance of neighboring ions. The angular dependence of the one-phonon process was satisfactorily described by a theory based on the angular dependence of the coupling between the ground and an excited quartet state due to the Zeeman interaction. From the angular-dependent results, it was possible to separate out the effect of the two possible local vibrations, E_g and T_{2g} , on the relaxation of the one-phonon process.

Although the absolute magnitude of the calculated relaxation rates are in good agreement with experiment, the variation of the relaxation rate between hosts was not as expected. In fact, the measured values of the matrix element of the orbit-lattice interaction for the T_{2g} -type vibrations for the one-phonon process and the matrix element for the two-phonon process increased with increasing lattice spacing in going from CaF₂ to BaF₂, whereas theory predicts a decrease. In addition, the experimental value of the matrix element of the orbit-lattice interaction for the one-phonon process for the E_g modes was essentially independent of the host. These discrepancies represent an inadequacy of the simple model presently being used to describe the relaxation process. In order to explain the discrepancy, the simple model can be changed to include such things as covalency, the nonisotropic nature of the lattice, shielding²⁵ of the crystal potential by the 5S and 5P electrons which is large for $L=2$ terms, and use of a more sophisticated model for the lattice oscillators. However, the recent work by Walker²⁶ on the effect of changes on the force constants due to the introduction of the impurity ion on the one-phonon relaxation process appears to be a most significant modification on the model. Undoubtedly this effect must be examined in greater detail in the future. However, these results show that indeed the simple model does predict the correct magnitude of the relaxation rate. But the model is not adequate to predict changes in the relaxation rate as the lattice is changed.

The experimental methods employed to perturb the population distribution of the spins and to measure the frequency dependence of the relaxation time by

²⁵ Gerald Burns, J. Chem. Phys. **42**, 377 (1965); A. K. Raychaudhuri and D. K. Ray, Proc. Phys. Soc. (London) **690**, 839 (1967).

²⁶ M. B. Walker, Can. J. Phys. **46**, 161 (1968).

both a fixed and continuous manner are of importance. These techniques can be applied to ions having a relatively simple ground state and having absorption bands which possess some paramagnetic circular dichroism. Using these methods, the frequency dependence of T_1 , which is very difficult to obtain when microwaves alone are used, can be measured on a number of crystals during a single experiment. In addition, some of the difficulties encountered in finding and studying cross-relaxation peaks can be eliminated by this approach.

These studies showed that the use of only temperature-dependent data when the ion is weakly coupled to the lattice can lead to an erroneous identification of the single-ion, one-phonon process. This implies that many of the reported magnitudes of T_1 for weakly coupled ions are not values of the single-ion, one-phonon process. The results given in this paper for the one-phonon process differ by three orders of magnitude from that reported for Tm^{2+} in CaF_2 . Also, the interpretation of the data²⁷ for Yb^{3+} in CaF_2 , SrF_2 , and BaF_2 on the one-phonon process is highly suspect. Tm^{2+} and Tb^{3+} are isoelectronic and their relaxation rates should be very similar.

ACKNOWLEDGMENTS

The authors wish to acknowledge their indebtedness to Dr. H. A. Weakliem for the use of his data prior to publication. We also wish to thank J. Beherrell for his assistance with the experiments.

APPENDIX: ANISOTROPY OF RELAXATION RATE FOR ONE-PHONON PROCESS FOR Tm^{2+} IN CUBIC CRYSTALS

For Kramer's doublets, relaxation is caused by the admixture of excited states into the ground doublet by the magnetic field. Any anisotropy²⁸ in the coupling between the ground and excited states will then be reflected in the relaxation rate. The relaxation rate is proportional to the matrix element given by

$$|M|^2 = \sum_{l,m} \left| \sum_i \langle E_{5/2}, +\frac{5}{2} | \mathbf{u} \cdot \mathbf{H} | G_{3/2}, i \rangle \times \langle G_{3/2}, i | V_l^m | E_{5/2}, -\frac{5}{2} \rangle \right|^2. \quad (\text{A1})$$

The appropriate energy level diagram is given in Fig. 13, where the $E_{5/2}$ state is lowest and the quartet G state is the only nearby excited state which has a nonzero matrix element. The two doublets are not mixed by a magnetic field. The magnetic dipole operation is $\mathbf{u} \cdot \mathbf{H}$ and V_l^m is the operator for the orbit-

²⁷ A. A. Antipin, A. N. Katyshev, I. N. Kurkin, and L. Ya. Shekun, *Fiz. Tverd. Tela* **9**, 3400 (1967) [English transl.: *Soviet Phys.—Solid State* **9**, 2684 (1968)].

²⁸ The anisotropy of the relaxation rate for Kramer's doublets in cubic crystals has also been calculated by Ray *et al.* The calculations are in agreement with each other. T. Ray and D. K. Ray, *Phys. Rev.* **164**, 420 (1967); Santosh Kumar and D. K. Ray, *ibid.* **164**, 424 (1967).

TABLE VI. Matrix elements of T_{2g} (top) and E_g (bottom) connecting doublet and quartet states.

$E_{5/2} \times T_2$		$G_{3/2}$			
		$ +\frac{3}{2}\rangle$	$ +\frac{1}{2}\rangle$	$ -\frac{1}{2}\rangle$	$ -\frac{3}{2}\rangle$
$ +\frac{5}{2}\rangle$	-1	1	0	0	0
$ +\frac{5}{2}\rangle$	2	0	$\sqrt{\frac{2}{3}}$	0	0
$ +\frac{5}{2}\rangle$	1	0	0	$\sqrt{\frac{1}{3}}$	0
$ -\frac{5}{2}\rangle$	-1	0	$\sqrt{\frac{1}{3}}$	0	0
$ -\frac{5}{2}\rangle$	2	0	0	$\sqrt{\frac{2}{3}}$	0
$ -\frac{5}{2}\rangle$	1	0	0	0	1
$E_{5/2} \times E$					
		$ +\frac{3}{2}\rangle$	$ +\frac{1}{2}\rangle$	$ -\frac{1}{2}\rangle$	$ -\frac{3}{2}\rangle$
$ +\frac{5}{2}\rangle$	0	0	0	0	1
$ +\frac{5}{2}\rangle$	2	0	-1	0	0
$ -\frac{5}{2}\rangle$	0	-1	0	0	0
$ -\frac{5}{2}\rangle$	2	0	0	1	0

lattice interactions. For cubic symmetry, we need only consider the representation T_{2g} and E_g for V_l^m .

The magnetic dipole operator is expanded and written as

$$\mathbf{u} \cdot \mathbf{H} = A J_0 \cos \theta + B [J_{-1} e^{i\phi} - J_1 e^{-i\phi}] \sin \theta,$$

where

$$A = \Lambda \beta H, \quad B = A/\sqrt{2}, \quad J_0 = J_z,$$

$$J_{-1} = (J_x - iJ_y)/\sqrt{2}, \quad J_1 = -[(J_x + iJ_y)/\sqrt{2}],$$

and J are the magnetic operators. To apply perturbation theory, it is necessary to use linear combinations of $|E_{5/2}, +\frac{5}{2}\rangle$ and $|E_{5/2}, -\frac{5}{2}\rangle$ that diagonalize the $E_{5/2}$ doublet in the presence of a magnetic field. The calculation can now be made in a simple and general way by using the coupling coefficients given by Polo.²² These show that the matrix elements of E_g and T_{2g} connecting a doublet and a quartet are as shown in Table VI.

Using Tables VI, the matrix element for E_g -type modes is given by

$$|M|^2 = \frac{1}{2} B^2 K_1^2 K_2^2 [\sin^2 2\theta + \sin^2 2\phi \sin^4 \theta], \quad (\text{A2})$$

where K_1 and K_2 are the reduced matrix elements for the magnetic dipole and E_g operators, respectively. The matrix element for T_{2g} vibrations is

$$|M|^2 = \frac{2}{3} B^2 K_1^2 K_3^2 [1 - \frac{1}{2} (\sin^2 2\theta + \sin^4 \theta \sin^2 2\phi)], \quad (\text{A3})$$

where K_3 is the reduced matrix element for the T_{2g} operator. The expected angular dependence of the relaxation rate for the one-phonon process due to the mixing of the ground doublet with a quartet state is in general described by the equation

$$W = W_{T_{2g}} + [W_{E_g} - \frac{1}{2} W_{T_{2g}}] S(\theta, \phi), \quad (\text{A4})$$

where $S(\theta, \phi) = \sin^2 2\theta + \sin^4 \theta \sin^2 2\phi$ and $W_{T_{2g}}$ and W_{E_g} are the relaxation rates along the $[100]$ direction for vibrations of T_{2g} symmetry and along the $[110]$ direction for modes of E_g symmetry. For the $[100]$ direction, $\theta = \phi = 0^\circ$, only modes of T_{2g} symmetry are nonzero. Note that the relaxation rate W can be independent of direction if $W_{E_g} = \frac{1}{2} W_{T_{2g}}$.